UNIVERSITY OF COPENHAGEN

KIC 1571511B

a benchmark low-mass star in an eclipsing binary system in the Kepler field

Ofir, A.; Gandolfi, D.; Buchhave, Lars A.; Lacy, C. H. S.; Hatzes, A. P.; Fridlund, Malcolm

KIC 1571511B: a benchmark low-mass star in an eclipsing binary system in the *Kepler* field[★]

A. Ofir,[1]† D. Gandolfi,[2,3] Lars Buchhave,[4,5] C. H. S. Lacy,[6] A. P. Hatzes[3] and Malcolm Fridlund[2]

[1]*School of Physics and Astronomy, Raymond and Beverly Sackler Faculty of Exact Sciences, Tel Aviv University, Tel Aviv 69978, Israel*
[2]*Research and Scientific Support Department, ESTEC/ESA, PO Box 299, 2200 AG Noordwijk, the Netherlands*
[3]*Thüringer Landessternwarte, Sternwarte 5, Tautenburg, D-07778 Tautenburg, Germany*
[4]*Center for Star and Planet Formation, Natural History Museum of Denmark, University of Copenhagen, DK-1350 Copenhagen, Denmark*
[5]*Niels Bohr Institute, Copenhagen University, DK-2100 Copenhagen, Denmark*
[6]*Department of Physics, University of Arkansas, Fayetteville, AR 72701, USA*

ABSTRACT

KIC 1571511 is a 14-d eclipsing binary (EB) in the *Kepler* data set. The secondary of this EB is a very low mass star with a mass of $0.14136 \pm 0.00036\,\mathrm{M_\odot}$ and a radius of $0.17831^{+0.00051}_{-0.00062}\,\mathrm{R_\odot}$ (statistical errors only). The overall system parameters make KIC 1571511B an ideal 'benchmark object': among the smallest, lightest and best-described stars known, smaller even than some known exoplanet. Currently available photometry encompasses only a small part of the total: future *Kepler* data releases promise to constrain many of the properties of KIC 1571511B to unprecedented level. However, as in many spectroscopic single-lined systems, the current error budget is dominated by the modelling errors of the primary and not by the above statistical errors. We conclude that detecting the RV signal of the secondary component is crucial to achieving the full potential of this possible benchmark object for the study of low-mass stars.

Key words: methods: data analysis – occultations – binaries: close – binaries: eclipsing.

1 INTRODUCTION

Current stellar models describe well the basic properties of a wide range of stars. However, there are persisting discrepancies at the lower end of the stellar mass range, where very late-type stars have measured radii that are higher than theory predicts (e.g. Lacy 1977; Torres & Ribas 2002; Ribas 2006). This Letter reports the discovery that *Kepler* target KIC 1571511 is an eclipsing binary (EB) which contains a very low mass star as secondary – hereafter just 511B – based on the public Q0-Q2 *Kepler* data and our radial velocity (RV) follow-up. We point out the special location of 511B in the parameter space and offer to use it as a benchmark object for future studies of low-mass stellar objects. In Section 2, we highlight the important properties of the KIC 1571511 photometry and subsequent RV follow-up, and in Section 3 we model the system. In Section 4, we estimate the system's physical parameters based on all available data, and conclude in Section 5.

2 IDENTIFICATION AND FOLLOW-UP

We identified KIC 1571511 as an interesting system as early as four days after the *Kepler* Q0-Q1 data were made public (Borucki 2010; see references therein for a description of the *Kepler* satellite and data). This system contains periodic eclipse-like events every 14.02 d, with a depth of ∼2 per cent – a conspicuous signal at *Kepler*'s high precision. At that time we suspected this system to host a giant transiting planet overlooked by the *Kepler* team due to its (assumed) orbital eccentricity. It is noteworthy that while high-eccentricity transiting planets can generate transits that are 'too' long and photometrically identical to EBs on a circular orbit, the *Kepler* pipeline does not consider eccentric orbits in its Data Validation module.[1] We thus were able to secure a few RV measurements with the Fibre-fed Echelle Spectrograph (FIES) at the Nordic Optical Telescope (NOT) observatory to test the giant-eccentric-planet hypothesis. We note that this object was also considered as an overlooked planetary candidate by Coughlin et al. (2010) but they did not provide RV data.

RV follow-up of KIC 1571511 was started in 2010 October using the FIES attached to the 2.61-m NOT (observing programme

---

[1] Kepler Data Processing Handbook section 9.3, document number KSCI-19081-001 of 2011 April 1.

HJD −245 0000	RV (km s^{-1})	RV error (km s^{-1})	$T_{\exp}$ (s)	S/N per pixel at 6000 Å
5479.36633498	−29.998	0.046	2700	26
5482.46744505	−10.181	0.042	2400	22
5484.50488456	−13.196	0.073	1500	12
5491.37000002	−29.871	0.054	1200	14
5497.32650926	−10.578	0.055	1200	16
5518.32931804	−27.713	0.060	1200	16

P41-426). The observations were performed under grey/dark time with good and stable sky conditions. The 1.3-µm high-resolution fibre was employed, yielding a resolving power of $\lambda/\Delta\lambda \approx 67\,000$ and a wavelength coverage of about 3600–7400 Å. Following the method described in Buchhave et al. (2010), long-exposed ThAr spectra were acquired immediately before and after each target spectrum to improve the wavelength solution and trace any instrumental drifts. Standard IRAF routines were used for the data reduction and spectra extraction. The RV measurements were derived by cross-correlating the target spectra with a spectrum of the RV standard star HD 182488 (Udry et al. 1999) observed with the same instrument set-up as the target. A journal of the FIES observations is given in Table 1. The FIES observations revealed a single-line spectroscopic binary (SB1) with an eccentric orbit ($e \cong 0.33$) and an RV semi-amplitude of $K \cong 10.5\,\mathrm{km\,s^{-1}}$, compatible with a very low mass companion star orbiting the main component. Fig. 1 (right-hand panels) shows the FIES RV measurements along with the Keplerian RV curve resulting from the best-fitting simultaneous photometric–RV solution (see Section 3) and residuals.
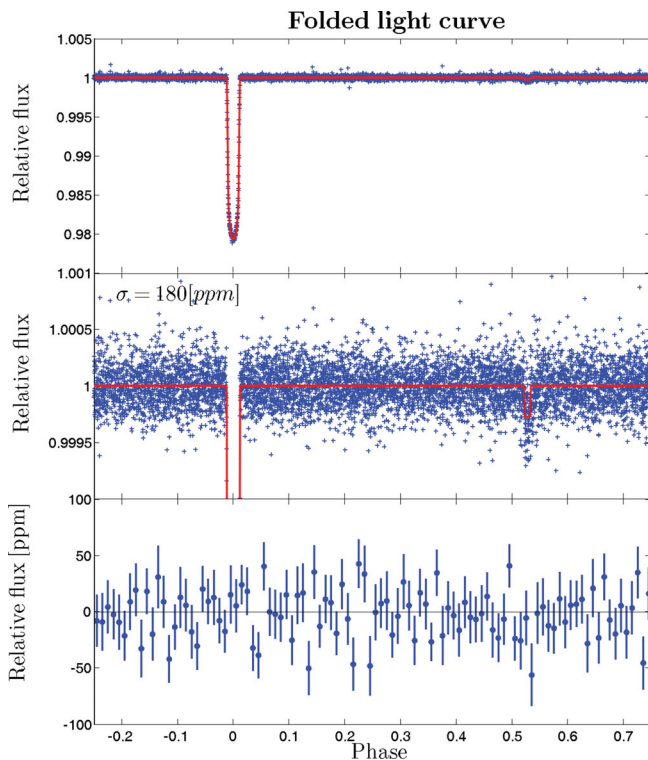
3 SYSTEM MODELLING WITH MCMC

3.1 Pre-processing

Since both the primary and secondary eclipses were easily identified using a weak filter, we were able to use a stronger filtering scheme for the final light curve (LC) without modifying the eclipses themselves. We computed an iterative ~1 d long, second-order Savitzky–Golay filter with 5σ outlier rejection using only the out-of-eclipses sections of the data, and separately for each continuous section of the Q0-Q2 data. We then interpolated the filter to the times of the eclipses and normalized the LC with that filter. No data points were rejected to this point, but only removed from the filter calculation, and this LC contained 6177 data points. Continuous sections were taken between quarters and anomalies, as reported by the *Kepler* Release Notes (we considered the following anomalies: attitude tweak, safe mode, Earth point and coarse point). We note that such a strong filter automatically removes any in-phase out of eclipse variation, such as the reflection effect or the Doppler boosting signal (Zucker et al. 2007). We chose a strong filter to better remove the stellar activity since it has higher amplitude than the Doppler boosting signal and since anyhow no further information is expected from it given our high-precision RV data. Once an initial solution was obtained (below), we rejected 22 points that deviated by more than 4σ from the model, and the data were used for the LC part of the final solution.

3.2 Methods

We used Monte Carlo Markov Chain (MCMC; e.g. Tegmark et al. 2004) for the simultaneous solution of the photometry and RV
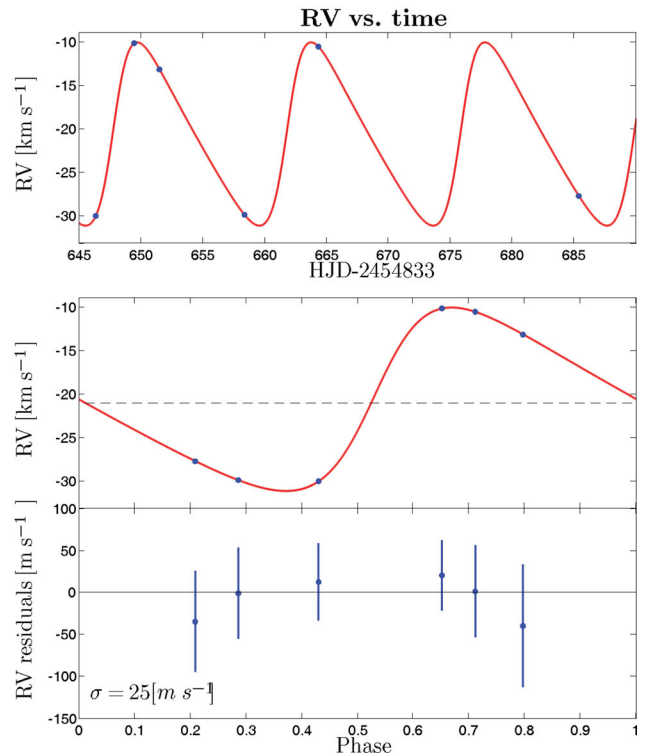
Figure 1. Result of the simultaneous RV–photometry solution. Left: the top panel shows the filtered and phased LC (blue) and the model (red), the middle panel gives a similar but expanded view, and the bottom panel includes the model residuals versus orbital phase binned to 1 per cent phase. Right: the measured RVs (blue) and the model (red) are depicted versus time (top panel), and phase (middle panel). The bottom panel gives the model residuals versus orbital phase. Note phase zero is defined at mid-transit, not at periastron passage.

data. As in many MCMC codes, an MCMC begins by computing the model for a given set of parameters. We then add a random perturbation to each parameter p chosen from normal distribution of width σ_p. If the total χ^2 has reduced at the new perturbed location, the perturbed parameters set is accepted as the new set. If the total χ^2 has increased, the new set is only sometimes accepted – at a probability of $\exp(\frac{\chi^2_{old} - \chi^2_{new}}{2})$, also commonly referred to as the Hastings–Metropolis jump condition. Early chains used a rather large σ_p, or step size, as the parameter space was explored for interesting regions of low χ^2. Once an initial solution was obtained, we set all the different jump sizes to the standard deviation of that MCMC test chain, and rescaled them down by a common factor of $N_{DOF}^{1/2}$, where $N_{DOF} = 13$ is the number of degrees of freedom. This is done since once all the parameters' jumps are measured in units of their own standard deviation, the MCMC process is actually a random walk in an N_{DOF}-dimensional space, and so the typical distance covered by such a step is $N_{DOF}^{1/2}$.

We use the above MCMC procedure and the Mandel & Agol (2002) formalism to model the system as two luminous spheres (versus Roche geometry models). We expand the formalism to account for the secondary's flux and *Kepler*'s finite integration time (Kipping 2010). Specifically, equation (40) of Kipping (2010) implied a subsampling of $N \simeq 2.3$ subsamples to reduce the modelling errors to below the measurement errors. We therefore chose $N = 5$ to make sure this effect is indeed minimized.

Our model included eccentric Keplerian orbits with a period P, a unit semimajor axis $a \equiv 1$, and eccentricity and argument of periastron given by $e\cos(\omega)$ and $e\sin(\omega)$. The fitted reference time parameter is the more easily (and more accurately) observed time of mid-eclipse T_{mid}, while the time of periastron passage is computed from it using the previous parameters. Other parameters are the fractional radius of the primary r_1/a, the relative radius of the secondary r_2/r_1 and the orbital inclination to the line of sight i. Using the Mandel & Agol (2002) limb-darkening model, we included a quadratic limb-darkening for the primary using $u_{1,1}$, $u_{2,1}$ and a linear limb-darkening for the secondary with $u_{1,2}$. Since the total flux is normalized to unity, we only varied the secondary fractional luminosity L_2/L_{tot}. When contamination, or 'third light' L_3, was included, contamination levels of more than ~ 3 per cent gave poorer fits, and contamination levels <3 per cent were just as good as the fit with zero contamination, so we adopted a fixed $L_3 = 0$. Finally, the mass ratio $q = \frac{m2}{m1+m2}$ affects the positions of the two bodies – and so it is included in the LC model too, and not just in the RV model. From the above, it follows that for the RV model we only needed to add the systemic velocity γ and the overall scale of the system – how many metres there are in one semimajor axis a. These are only a shift and scaling terms for the otherwise known RV morphology (from the previous parameters). In principle, the scaling parameter should be an MCMC variable and the systemic velocity should be fitted analytically – but since this is a single-lined binary, the scale is degenerate with the mass ratio. We therefore did not vary the scaling parameter but fixed at a value computed from the estimated mass of the primary (Section 4), the above period and mass ratio, and Kepler's laws.

3.3 Application to KIC 1571511

We searched the above parameter space using numerous MCMC until we got very close (in retrospect – within $\Delta\chi^2 < 5$) to the absolute χ^2 minimum. We then ran 30 chains of 5×10^4 steps each to densely sample the local volume. We verified that all of them

converged on the same parameters set and then concatenated all the chains (as they are independent; see Tegmark et al. 2004) to a final 1.5×10^6 steps long chain used for the parameters value and errors estimation. We also checked that all parameters are well mixed, i.e. their effective length (which is their nominal length divided by their autocorrelation length) is $\gg 1$. Since we started all the runs from a point very near to the final minimum, no 'burn-in' was required and all steps were kept. To further check that no farther and deeper minima exist, we also ran 300 shorter chains that did not start from near the reported χ^2_{min} – but randomly perturbed by up to 100σ in every parameter. No other deeper minimum was found. The best-fitting parameters and their errors were determined as the median values of each parameter's distribution and the ranges that span 68.3/2 per cent of the steps on either side of that median. These parameters and errors, as well as some derived quantities, are reported in Table 3 and the LC and RV models are shown in Fig. 1.

Overall the quality of the fit is satisfactory, with χ^2_{tot} of 8046.5, or reduced χ^2_{red} of 1.31. Some of the excess residuals can be attributed to imperfect filtering of microactivity on primary: the EB is active with an amplitude of 7.2×10^{-4}, while the LC residuals are 1.8×10^{-4} – almost four times lower. It is unlikely that this variability is dominated by 511B since this would imply a variability of about 25 per cent in its flux on $\sim$day time-scales, and so we attribute it almost entirely to the primary (hereafter just 511A). It is noteworthy that while both limb-darkening coefficients of 511A were constrained by the data, no such constraint is yet possible even for the simplest linear model of 511B.

4 PHYSICAL PARAMETERS ESTIMATION

Single-lined spectroscopic and eclipsing binaries, such as KIC 1571511, do not allow for the full model-free determination of their parameters. The derived quantities can only be solved up to a single line of possible mass/radius relations for each one of the components (Beatty et al. 2007, hereafter B07). One therefore needs to derive the primary's mass from some models, and systematic errors at this stage are the overwhelming source of error for this data set (more below). We therefore took extra care and used multiple tools redundantly for the following step. We modelled the co-added FIES spectrum of 511A primarily using the new SPC fitting scheme (Buchhave et al., in preparation) which allowed us to extract precise stellar parameters from the spectrum (see Table 2). We double checked this new analysis with the more traditional spectral synthesis package SME (Valenti & Piskunov 1996; Valenti & Fischer 2005) and got a similar and consistent results. We then used T_{eff}, $\log(g)$ and Fe/H and a grid of Yonsei–Yale model isochrones (Yi et al. 2001), and performed a Monte Carlo analysis to infer the stellar mass and radius and an estimate of their uncertainties. This yielded a stellar mass and radius of $M_{511A} = 1.265^{+0.036}_{-0.030}\,M_\odot$ and $R_{511A} = 1.216^{+0.165}_{-0.043}\,R_\odot$, respectively. Since the radius of 511A can also be inferred from the above mass and the observationally constrained relation of B07, and since the latter gives lower errors, we adopt its values: $R_{511A} = 1.343^{+0.012}_{-0.010}\,R_\odot$. We note that at this stage we effectively have three different determinations for the primary's

Table 2. Photospheric parameters of KIC 1571511A as derived from the spectral analysis of the co-added FIES spectrum.

T_{eff}(K)	$\log(g)$ (cm s^{-2})	Fe/H (dex)	$v\sin i$ (km s^{-1})
6195 ± 50	4.53 ± 0.10	0.37 ± 0.08	7.9 ± 0.5

surface gravity: one [$\log(g) = 4.53$] comes directly from the spectral analysis, and the other two are indirect from the combination of mass and radius from the above Monte Carlo distribution [$\log(g) = 4.37$] and B07 relation [$\log(g) = 4.28$]. We choose to adopt this last determination because it is least model-dependent: given the primary's mass, it only assumes Kepler's laws and spherical stars.

511B is thus determined to have a mass of $0.14136 \pm 3.6 \times 10^{-4}; \, ^{+51}_{-42} \times 10^{-4} \, \mathrm{M_\odot}$ and a radius of $0.17831^{+5.1}_{-6.2} \times 10^{-4}; \, ^{+13}_{-16} \times 10^{-4} \, \mathrm{R_\odot}$ (statistical and modelling errors, respectively). Not surprisingly, both the LC and the RV data are far more precise than the model-dependent derivation of the mass of 511A, and the latter is the overwhelming source of error in the derived physical parameters of 511B. We therefore quote two error estimations of the mass and radius of 511B in Table 3 – the larger is derived only from the modelling error of the mass of 511A, and the smaller is derived only from statistical errors of the LC–RV fit.

Since we did not model the reflection effect, the $L_2/L_{\mathrm{tot}} = 2.75 \times 10^{-4}$ depth of the secondary eclipse is a combination of the primary's flux reflected off the secondary and of the intrinsic luminosity of 511B itself. The former can be calculated as $F_{\mathrm{reflected}} = A_g \left(\frac{r_2}{a}\right)^2 \sin(i)$, where A_g is the geometric albedo and a is the primary–secondary distance during secondary eclipse, which in this case is $F_{\mathrm{reflected}} = A_g \times 4.2 \times 10^{-5}$. We find that reflected light cannot contribute more than about 1/6 of the light lost during the secondary eclipse. Thus, at least 2.33×10^{-4} (and probably much closer to the entire 2.75×10^{-4}) of the total flux in the *Kepler* passband can be attributed to 511B's intrinsic luminosity. A toy model[2] (using a uniform *Kepler* passband between 420 and 900 nm and blackbody spectral densities) gives a temperature range for 511B of $T_{\mathrm{eff,511B}} = 4030$–$4150$ K for the above contrast range.

5 DISCUSSION

We present the initial characterization of *Kepler* EB KIC 1571511. We show that the secondary of this EB is a very low mass star with a mass of $0.14136 \, \mathrm{M_\odot}$ and a radius of $0.17831 \, \mathrm{R_\odot}$ – so its diameter is smaller than some planet (e.g. Anderson et al. 2011b; Hartman et al. 2011). For a low-mass object to be considered for a 'benchmark status' of its class, one would want that the object would be physically associated with a more Sun-like star, since such stars are currently better understood. Better still are such binaries that are eclipsing, and the best constraints could come from such fully eclipsing and double-lined binaries, where masses and radii are arrived at model-free. KIC 1571511 is almost such an EB – currently lacking only the secondary's RV signal. Indeed, if one plots the uncertainty in mass and radius of all well-characterized (both errors under 5 per cent) low-mass objects and of 511B (Fig. 2), it is easy to see that the latter occupies a unique spot of the lowest mass well-characterized star just above the brown dwarfs (BDs) to stars transition ($0.075 \, \mathrm{M_\odot}$). Importantly, the overwhelming source of error on both the mass and radius of 511B is the error on the mass of the primary, 511A. This is due, on the one hand, to the single-lined nature of the system in the visible band and, on the other hand, to the exquisite quality of the *Kepler* LC which allows for very precise determination of all LC-derived quantities. This, in turn, means that the continued *Kepler* observations on the target guarantee marked improvements in all LC-derived quantities in the future, while any

[2] See Kepler Instrument Handbook, document KSCI-19033, for full description.

Table 3. The best-fitting model of the KIC 1571511 system and derived quantities. The overwhelming error source on the physical parameters is the error on M_1 due to the SB1 nature of the system – so the derived errors are computed twice: with M_1 modelling errors included (marked with an asterisk) and without (statistical error only).

Parameter	Value	Error	Unit
Fitted LC parameters			
P	14.022480	$^{+2.3}_{-2.1} \times 10^{-5}$	d
T_{mid}	4968.527088	$^{+8.9}_{-9.9} \times 10^{-5}$	$\mathrm{HJD} - 245\,0000$
r_1/a	0.04891	$\pm 3.1 \times 10^{-4}$	
r_2/r_1	0.13277	$^{+3.8}_{-4.6} \times 10^{-4}$	
i	89.480	$^{+0.069}_{-0.056}$	$^\circ$
$e\cos(\omega)$	-0.04057	$\pm 4.0 \times 10^{-4}$	
$e\sin(\omega)$	0.3244	$^{+2.8}_{-2.6} \times 10^{-3}$	
L_2/L_{tot}	2.75×10^{-4}	$\pm 0.19 \times 10^{-4}$	
$u_{1,1}$	0.373	± 0.019	
$u_{2,1}$	0.205	$^{+0.047}_{-0.045}$	
$u_{1,2}$	0.43	$^{+0.38}_{-0.30}$	
$q = \frac{m_2}{m_1+m_2}$	0.10052	$\pm 2.3 \times 10^{-4}$	
L_3/L_{tot}	0	(fixed)	
Fitted RV parameters			
γ	-21030.2	± 3.7	$\mathrm{m\,s^{-1}}$
Scale	1.265	(fixed)	$\mathrm{M_\odot}$ (M_1 model)
Derived parameters			
K	10521	± 24	$\mathrm{m\,s^{-1}}$
e	0.3269	± 0.0027	
b	0.383	$^{+0.040}_{-0.049}$	
ω_1	82.872	± 0.099	$^\circ$
ρ_1	740	± 14	$\mathrm{kg\,m^{-3}}$
	0.5242	$\pm 9.9 \times 10^{-3}$	$\rho_\odot$
$\log g_2$	5.0875	$^{+8.0}_{-7.6} \times 10^{-3}$	$\mathrm{cm\,s^{-2}}$
Mass function	142.8×10^{-5}	$\pm 1.02 \times 10^{-5}$	$\mathrm{M_\odot}$
Physical parameters			
M_1	1.265	$^{+0.036}_{-0.030}$	$\mathrm{M_\odot}$ (from model)
M_2	0.14136	$\pm 3.6 \times 10^{-4}$	$\mathrm{M_\odot}$
		$^{+51}_{-42} \times 10^{-4}$	$\mathrm{M_\odot}$ *
R_1	1.343	$^{+0.012}_{0.010}$	$\mathrm{R_\odot}$
R_2	0.17831	$^{+5.1}_{-6.2} \times 10^{-4}$	$\mathrm{R_\odot}$
		$^{+13}_{-16} 10^{-4}$	$\mathrm{R_\odot}$ *
$T_{\mathrm{eff,511B}}$	4030–4150	(see text)	K

observation of the system as an SB2 (perhaps in the infrared) will dramatically reduce the overall error on both the mass and radius of 511B. This is visualized with the empty symbol of 511B in Fig. 2 which shows that discounting the (modelling) error on the mass of 511A drastically reduces the errors on the parameters of 511B to potentially the best characterized and lowest mass object – so a potential benchmark object indeed.

When compared with other known low-mass stars, all the other systems we encountered are less favourable to serving as benchmarks of this kind: most known late M dwarfs and BDs are not in eclipsing systems at all. Nearly all low-mass EBs, and especially those observed from the ground, have LCs that cannot compete with
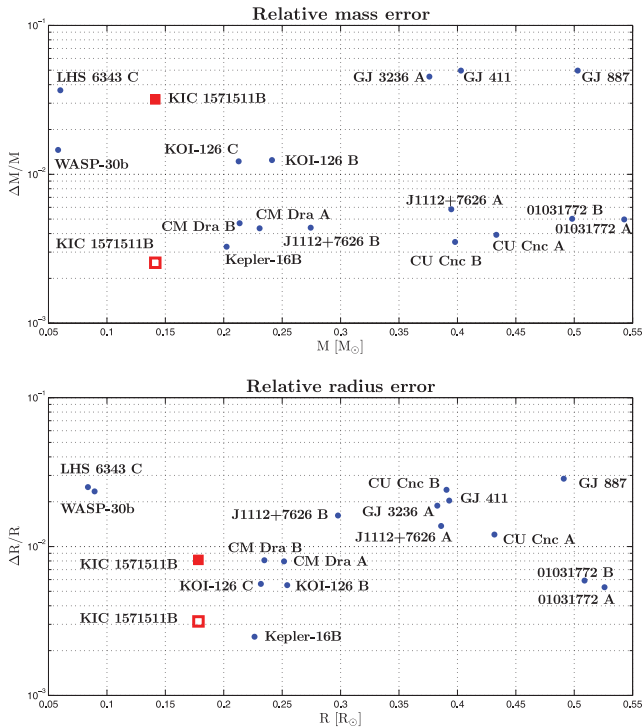
Figure 2. Relative precision of the mass (upper panel) and radius (lower panel) of all well-characterized low-mass stars (M$_\star$ < 0.55M$_\odot$) with both determined to better than 5 per cent (blue circles). Also noted (red square) is the location of KIC 1571511B - once derived only from the error on the mass of 511A (filled symbol) and once derived only from statistical errors (empty symbol). References: LHS 6343 C (Johnson et al. 2011), WASP-30b (Anderson et al. 2011a), KOI-126 B,C (Carter et al. 2011), CM Dra A & B, CU Cnc A & B, GJ 411, GJ 887 (López-Morales 2007 and references therein), GJ 3236 A (Irwin et al. 2009), LSPM J1112+7626 A and B (Irwin et al. 2011), Kepler-16B (Doyle et al. 2011)

Kepler's exquisite quality. However, there are a number of other interesting objects already in that data set: KOI-126 B,C (Carter et al. 2011) and Kepler-16B (Doyle et al. 2011) are indeed very low mass stars – but all are part of compact hierarchical triple systems, making follow-up and analysis more difficult. We conclude that KIC 1571511B is indeed uniquely situated to become a benchmark object for the study of low-mass stars.

REFERENCES

Anderson D. R. et al., 2011a, ApJ, 726, L19
Anderson D. R. et al., 2011b, MNRAS, 416, 2108
Beatty T. G. et al., 2007, ApJ, 663, 573 (B07)
Borucki W. J. (for the Kepler Team 2010), preprint (arXiv:1006.2799)
Buchhave L. A. et al., 2010, ApJ, 720, 1118
Carter J. A. et al., 2011, Sci, 331, 562
Coughlin J. L., López-Morales M., Harrison T. E., Ule N., Hoffman D. I., 2011, AJ, 141, 78
Doyle L. R. et al., 2011, Sci, 333, 1602
Enoch B., Collier Cameron A., Parley N. R., Hebb L., 2010, A&A, 516, A33
Hartman J. D. et al., 2011, ApJ, 742, 59
Irwin J. et al., 2009, ApJ, 701, 1436
Irwin J. M. et al., 2011, ApJ, 742, 123
Johnson J. A. et al., 2011, ApJ, 730, 79
Kipping D. M., 2010, MNRAS, 408, 1758
Lacy C. H., 1977, ApJS, 34, 479
López-Morales M., 2007, ApJ, 660, 732
Mandel K., Agol E., 2002, ApJ, 580, L171
Ribas I., 2006, Ap&SS, 304, 89
Southworth J., Maxted P. F. L., Smalley B., 2004a, MNRAS, 351, 1277
Southworth J., Zucker S., Maxted P. F. L., Smalley B., 2004b, MNRAS, 355, 986
Tegmark M. et al., 2004, Phys. Rev. D, 69, 103501
Torres G., Ribas I., 2002, ApJ, 567, 1140
Udry S., Mayor M., Queloz D., 1999, in Hearnshaw J.B, Scarfe C. D., eds, IAU Colloq. 170, ASP Conf. Ser. Vol. 185, Precise Stellar Radial Velocities. Astron. Soc. Pac., San Francisco, p. 367
Valenti J. A., Piskunov N., 1996, A&AS, 118, 595
Zucker S., Mazeh T., Alexander T., 2007, ApJ, 670, 1326

This paper has been typeset from a TEX/LATEX file prepared by the author.